Thermodynamic Study of the Binding of Methyltrioxorhenium with Pyridine and Its Derivatives in Benzene Solution

S. Masoud Nabavizadeh,*[a] Alireza Akbari,[a] and Mehdi Rashidi[a]

Keywords: N ligands / Rhenium / Thermodynamics

A spectrophotometric study of the interaction of methyltrioxorhenium (MTO) with pyridine and its derivatives in benzene solution has been carried out at various temperatures. The stability constants of the resulting 1:1 complexes were determined by analysis of spectrophotometric data and found to vary in the order 3,4-Me_2Py > 4-*t*BuPy > 4-MePy > 3-MePy > 4-BenzylPy > Py > 3-PhPy > 3-C(O)OMePy > 3-ClPy. The enthalpy and entropy of adduct formation were determined from the temperature dependence of the stability constants. All complexes formed were enthalpy stabilized but entropy destabilized.

Introduction

Methyltrioxorhenium (MTO) has found numerous applications in various catalytic processes, especially the oxidation of olefins,[1,2] alcohols,[3,4] arenes[5] and carbonylmetal compounds.[6,7] Epoxidations with MTO/H_2O_2 has several advantages. For instance, MTO is easily available and is active at low concentrations of both MTO and H_2O_2. It works within a broad temperature range (–40 to +90 °C) and is stable in aqueous acidic solution as well as in basic media in special cases. Furthermore, the MTO/H_2O_2 system works in a broad variety of solvents, ranging from highly polar solvents (e.g. nitromethane, water) to solvents with low polarity (e.g., toluene). A major advantage of MTO, however, is that it does not decompose hydrogen peroxide. The most important drawback of the MTO-catalyzed process is the concomitant formation of diols instead of the desired epoxides, especially in the case of more sensitive substrates.[8] It has been reported that the use of Lewis base adducts of MTO significantly decreases the formation of diols due to the reduced Lewis acidity of the catalyst system. It has also been found that addition of a significant excess of pyridine as Lewis base not only hampers the formation of diols but also increases the reaction velocity in comparison to MTO as catalyst precursor.[9,10] In addition, it has been shown that 3-cyanopyridine, and especially pyrazole, as Lewis bases are even more effective and less problematic than pyridine itself, while pyridine *N*-oxides are less efficient.[11–14] The Brønsted basicity of pyridines lowers the activity of hydronium ions, thus reducing the rate of opening of the epoxide ring.[15] MTO forms trigonal-bipyramidal adducts with monodentate N-bases and (distorted) octahedral adducts with bidentate Lewis bases.[16–19] MTO and its monodentate Lewis base adducts react with H_2O_2 to form mono- and bisperoxo complexes. The activity of the bisperoxo complexes (with coordinated Lewis base) in olefin epoxidation depends on the nature, concentration, and redox stability of the Lewis bases. High selectivity (epoxide vs. diol) can be attained by temperature control, trapping of water, or the use of certain additives, such as aromatic Lewis-base ligands, which additionally accelerate the epoxidation reactions.[20] The pK_a of the Lewis base used is important in achieving ligand-accelerated catalysis since the extent of interaction between rhenium and the Lewis base can be correlated to the latter's pK_a: more basic Lewis bases tend to deactivate the MTO.[21] In this regard, we have recently presented a convincing correlation between log *K* of the binding constant, *K*, of the ligand L to MTO and the pK_a of L.[19] Considering the important applications of the pyridine–MTO complexes in catalytic processes, and the effect of temperature on olefin epoxidation, in the present work we have obtained the stability constants of adduct formation of MTO with pyridine derivatives at different temperatures and studied their thermodynamics.

[a] Department of Chemistry, College of Sciences, Shiraz University,
Shiraz, 71454, Iran
Fax: +98-711-228-6008
E-mail: nabavi@chem.susc.ac.ir

Results and Discussion

Adduct Formation with Electron Donors

(η^1-Organo)rhenium(VII) trioxides are Lewis acids with two free coordination sites. Reaction with Lewis bases leads to electronic and steric saturation of the Re center. Ligands, especially those with oxygen or nitrogen donor atoms, form Lewis acid–base adducts with MTO.[22–25] Although both sites of bidentate ligands, such as 2,2′-bipyridine, can bind

  DOI: 10.1002/ejic.200500004

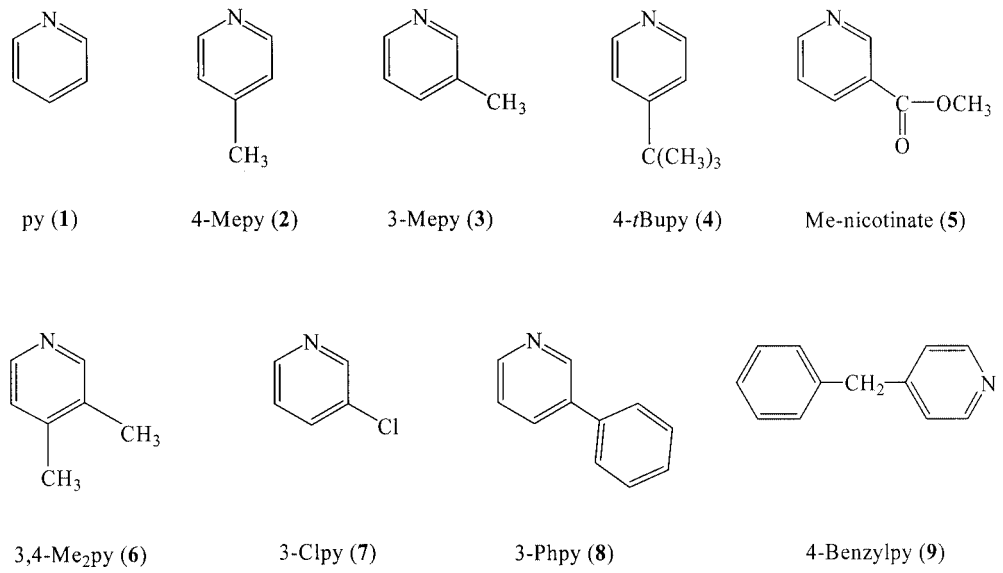

Scheme 1. Structural formulae of pyridine and its derivatives.

to the rhenium center to form a distorted octahedral complex,[26] usually only a single monodentate ligand coordinates to the rhenium atom when a monodentate ligand is used. The lack of formation of MTO·L_2 (L = monodentate ligands) is probably caused by steric factors. Adducts of the composition MTO·L_2 are only known for very small Lewis bases, for example NH_3.[24,25] Special attention has been paid to these adducts because they have proven to be highly selective oxidation catalysts.[23] The reaction of MTO with various pyridine derivatives in benzene affords 1:1 adducts of the composition [CH_3ReO_3]·N [N = pyridine (**1**), 4-picoline (**2**), 3-picoline (**3**), 4-*tert*-butylpyridine (**4**), methyl nicotinate (**5**), 3,4-dimethylpyridine (**6**), 3-chloropyridine (**7**), 3-phenylpyridine (**8**), and 4-benzylpyridine (**9**); see Scheme 1].

The interaction between MTO and several pyridines at different temperatures was studied by UV/Vis spectroscopy. The reaction between MTO and pyridines produces the indicated adduct; the crystal structure for the 4-*tert*-butyl analog has been reported previously.[16] In solution, however, these reactions do not proceed to completion. With UV/Vis detection, an increase in N-donor concentration caused more adduct to form. A series of experiments was carried out with various pyridine derivatives containing substitution in the 3- or 4-position. The values of the stability constants at different temperatures were evaluated for the reaction represented in Scheme 2.

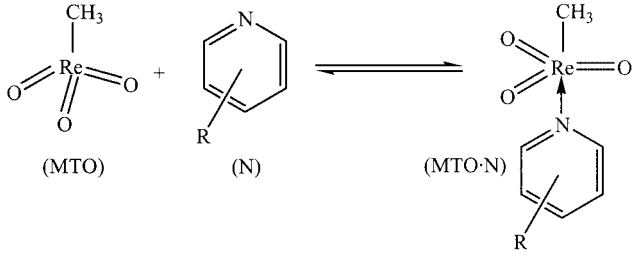

Scheme 2.

The corresponding stability constant, K_{eq}, is given by Equation (1).

$$K_{eq.} = \frac{[MTO{\cdot}N]}{[MTO][N]} \quad (1)$$

where [MTO·N], [MTO], and [N] represent the equilibrium molar concentrations of adduct (CH_3ReO_3·N), free MTO, and free (uncomplexed) pyridine or other ligand, respectively. The absorbance changes in the UV/Vis spectra were analyzed by a nonlinear least-squares fitting according to Equation (2):[19]

$$Abs_{eq} = \frac{\varepsilon_{MTO}([MTO]+[MTO{\cdot}N]) + \varepsilon_{MTO{\cdot}N} K_{eq}[N]([MTO]+[MTO{\cdot}N])}{1+K_{eq}[N]} \quad (2)$$

where Abs_{eq} is the absorbance of a solution at equilibrium, and ε_{MTO} and $\varepsilon_{MTO{\cdot}N}$, are molar absorptivities for the MTO and MTO·N species at the corresponding wavelength. The data for pyridine fit well to Equation (2), affording these values for the parameters: K_{eq} = 677.6 ± 9.7 L mol^{-1} and $\varepsilon_{MTO{\cdot}py}$ = 964.4 ± 2.7 L mol^{-1} cm^{-1} in benzene at 20 °C. Figure 1 shows the fit to Equation (2) of the absorbance values at corresponding wavelength for pyridine at different temperatures.

Derivatives of pyridine [4-Me, 3-Me, 4-C(CH_3)$_3$, 3-C(O)OMe, 3,4-Me_2, 3-Cl, 3-Ph and 4-CH_2Ph] also interact with MTO to a greater or lesser extent. These data were also treated by the same procedure used for pyridine. The resulting parameters are indicated in Table 1.

As shown before,[19] stability constants are sensitive to both steric and electronic effects. For N-donor ligands, a linear relationship between log K_{eq} and pK_a at given temperature is expected, as expressed by Equation (3).

$$\log K_{eq} = m(pK_a) + b \quad (3)$$

Table 1. Stability constants[a] for the coordination of substituted pyridines to MTO at different temperatures in benzene.

Entry	Ligand	K_{eq} [L mol^{-1}] at 10 °C	K_{eq} [L mol^{-1}] at 20 °C	K_{eq} [L mol^{-1}] at 30 °C	K_{eq} [L mol^{-1}] at 40 °C	pK_a[b]	σ[c]
1	pyridine	**1036.7 ± 34.1**	**677.6 ± 9.7**	**408.4 ± 5.0**	**250.6 ± 6.4**	5.23	0
2	4-picoline	**2056.8 ± 76.5**	**1248.8 ± 38.5**	**791.5 ± 6.9**	**510.9 ± 5.0**	5.89	–0.17
3	3-picoline	**2020.2 ± 188.6**	**1082.7 ± 53.1**	**696.5 ± 38.6**	**408.7 ± 13.6**	5.79	–0.07
4	4-*tert*-butylpyridine	**2542.9 ± 68.5**	**1637.9 ± 156.5**	**1043.5 ± 22.0**	**724.7 ± 14.2**	5.99	–0.20
5	methyl nicotinate	**220.8 ± 6.7**	**117.3 ± 3.3**	**66.5 ± 6.7**	**39.7 ± 2.8**	3.13	0.32
6	3,4-dimethylpyridine	**2848.6 ± 102.2**	**2082.5 ± 162.7**	**1698.7 ± 90.4**	**888.2 ± 89.2**	6.46	–0.24[d]
7	3-chloropyridine	**171.4 ± 7.6**	**89.0 ± 2.2**	**46.2 ± 3.5**	**29.1 ± 2.6**	2.84	0.37
8	3-phenylpyridine	**831.8 ± 7.2**	**494.3 ± 8.9**	**293.8 ± 4.7**	**185.4 ± 5.2**	4.80	0.06
9	4-benzylpyridine	**1649.5 ± 39.6**	**980.4 ± 42.9**	**537.2 ± 37.4**	**312.7 ± 19.6**	5.59	[e]
10	3,5-dibromopyridine	32.9	15.2	6.7	4.3	0.82	0.78[d]
11	4-$Me_2NC_5H_4N$	39219.3	33250.6	26921.6	17382.0	9.61	–0.83
12	3,5-dichloropyridine	29.1	13.3	5.8	3.8	0.67	0.74[d]
13	3-fluoropyridine	186.0	99.7	51.0	32.9	2.97	0.34
14	3-cyanopyridine	54.6	26.4	12.2	7.8	1.45	0.56
15	4-cyanopyridine	76.0	37.7	17.9	11.6	1.86	0.66
16	3-iodopyridine	233.1	127.4	66.4	42.9	3.25	0.35
17	4-phenylpyridine	1487.6	952.8	582.8	376.3	5.55	–0.01
18	3-methoxypyridine	866.9	530.1	309.6	199.9	4.88	0.12
19	4-methoxypyridine	3523.7	2429.9	1600.3	1033.2	6.62	–0.27
20	4-phenoxypyridine[f]	4653.7	3470.6	2423.3	1483.2	[g]	–0.32
21	3-acetylpyridine	220.3	119.8	62.2	40.2	3.18	0.38
22	4-acetylpyridine	287.4	159.9	84.9	54.8	3.51	0.50
23	3-aminopyridine	2190.3	1450.2	916.8	591.9	6.03	–0.16
24	4-aminopyridine	26212.0	21468.4	16791.9	10841.8	9.11	–0.66
25	3-pyridinecarboxyaldehyde[f]	319.9	188.3	101.2	62.7	[g]	0.25
26	4-pyridinecarboxyaldehyde	242.6	133.0	69.6	44.9	3.30	0.45
27	3-nitropyridine	32.6	15.1	6.6	4.3	0.81	0.71
28	4-nitropyridine	62.2	30.3	14.1	9.1	1.61	0.78
29	3-bromo-5-methoxypyridine	138.1	72.1	35.9	23.2	2.60	0.51[d]
30	3-methyl-4-nitropyridine	101.6	51.7	25.1	16.2	2.22	0.71[d]
31	4-amino-3-bromopyridine	4943.1	3509.1	2379.1	1536.0	7.04	–0.27[d]

[a] Experimental values are given in bold; the others are redundant values calculated from them at a given temperature according to Equation (3). [b] K_a applies to the reaction $HL^+ \rightleftharpoons H^+ + L$ in aqueous solution. Data are from ref.[27,28]. [c] The σ_m parameter was used for substitution at C(3), and the σ_p parameter was used for substitution at C(4). [d] These substituent parameters were obtained by adding the individual σ_m or σ_p values for both substituents. [e] Not defined. [f] Values of K_{eq} for these N-donor ligands were calculated with the Hammett equation [log $(K/K_0) = \rho\sigma$]. [g] Not known.

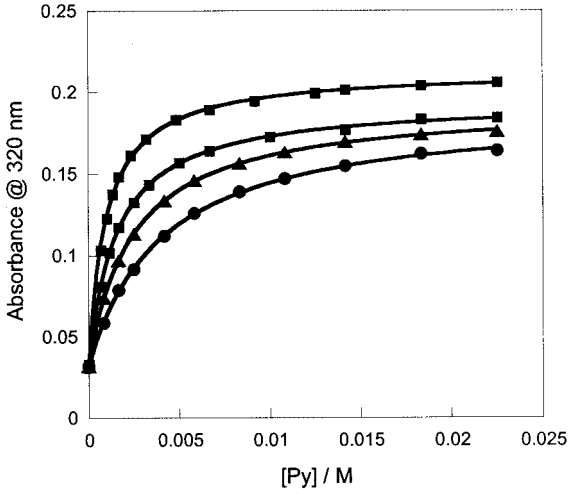

Figure 1. Change in absorbance at 320 nm on addition of pyridine (**1**) to MTO in benzene at T = 10, 20, 30, and 40 °C (temperature increases reading downward); the solid lines show the fit of the spectrophotometric data to Equation (2).

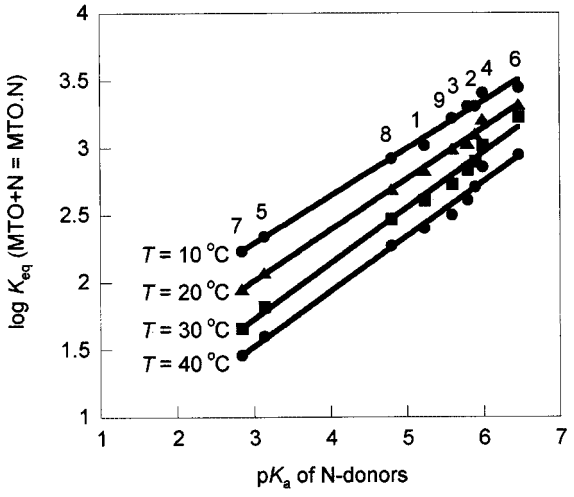

Figure 2. Plot showing a correlation between the stability constants (on the logarithmic scale) for adduct formation of MTO with different N-donors in benzene and pK_a of the same ligands.

In Figure 2, the values from Table 1 for log K_{eq} are plotted against pK_a at various temperatures. It is evident that the data for MTO·N fit on a straight line. The experimental results listed in Table 1 were used to calculate the straight-line equations summarized in Table 2 by least-squares procedures. These equations allow calculation of the expected stability constant for an adduct of any monodentate N-donor ligand from its pK_a. In Table 1, 36 values of K_{eq} at different temperatures are derived from experiments and the remaining 88 values of K_{eq} are redundant and were calculated directly from these 36 experimental values; of course, the calculated ones will have higher error limits owing to the propagation of errors.

Table 2. Straight-line correlations for stability constants of MTO with monodentate N-donors and ligand basicities[a] at different temperatures in benzene.

Temp. [°C]	m	b	R[b]
10	0.35 ± 0.01	1.23 ± 0.06	0.992
20	0.38 ± 0.01	0.87 ± 0.04	0.997
30	0.41 ± 0.02	0.49 ± 0.07	0.992
40	0.41 ± 0.02	0.30 ± 0.09	0.989

[a] The slopes (m) and intercepts (b) for the straight reference lines from plots of log K_{eq} vs. pK_a were calculated by the least-squares procedure from the data listed in Table 1. [b] Correlation coefficient.

From Table 1, it is obvious that the MTO–ligand interaction is considerably weakened at higher temperatures. The pyridine adducts of MTO are considerably less stable towards moisture and temperature than MTO itself. This enhanced sensitivity has also been observed for other N-donor adducts of MTO.[29]

Linear Free-Energy Relationship (LFER)

An attempted linear free-energy relationship (LFER) correlation according to the Hammett equation at 20 °C is displayed in Figure 3. The slopes of the line of log (K/K_0) vs. σ (substituent constant) are –2.04 ± 0.14 (R = 0.985), –2.22 ± 0.09 (R = 0.986), –2.42 ± 0.11 (R = 0.987) and –2.41 ± 0.07 (R = 0.992) at T = 10, 20, 30, and 40 °C, respectively, which are the reaction constants (ρ). The ρ values for these plots have an absolute magnitude greater than 1, thus indicating that the equilibrium is more sensitive to electronic effects than ionization of benzoic acid. The negative reaction constant for the pyridines' equilibrium indicates that a positive charge develops on the pyridine nitrogen in the adduct as compared with the free molecule. As expected, the Re^{VII} center acts as an electron acceptor, attracting electrons upon coordination. MTO is believed to be a hard Lewis acid on the basis of its strong interactions with N- and O-donor ligands and its weak interaction with S-donor ligands.[15] Therefore, the affinity for the hard N-atom in the N-donor ligands investigated here is expected to be quite high.

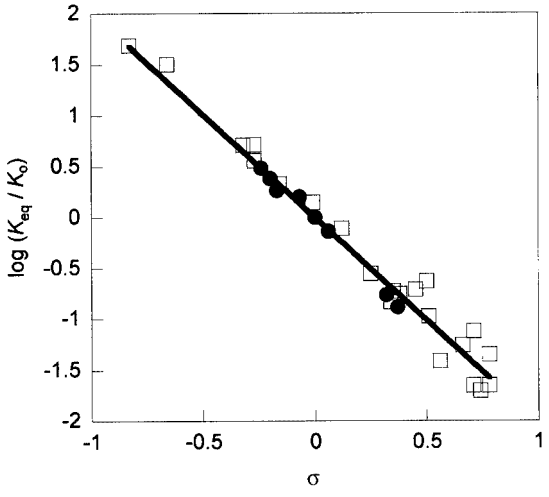

Figure 3. Hammett plot based on the stability constants (●: experimental values; □: calculated values) for the binding of substituted pyridines to MTO in benzene at 20 °C. The reaction constant (for ligands **1**–**9**) is –2.22 ± 0.09.

Effect of Donor

In this work, we have nine donors with different electron-donating capabilities due to different substitution on pyridine. We chose to examine only adducts with pyridines substituted in the *p*- and *m*- positions in order to minimize the steric influence of the Lewis base on the adducts. It is believed that the interaction between MTO and these donors is governed by the electron density on the nitrogen atom of the pyridine ring. On the basis of this description, the following sequence was confirmed from ΔG (20 °C, from Table 3) and K_{eq} (20 °C) values for the interaction of MTO with monodentate N-donors.

	MTO+(**5**)	MTO+(**1**)	MTO+(**4**)
K_{eq} (20 °C) /L mol^{-1}	117.3	677.6	1637.9
ΔG (20 °C) /kJ mol^{-1}	–11.6	–15.9	–18.1

Thermodynamic Parameters

In order to have a better understanding of the thermodynamics of adduct-formation reactions of monodentate N-donors with MTO, it is useful to consider the enthalpic and entropic contributions to these reactions. The ΔH and ΔS values for the adduct formation reactions were evaluated from the corresponding temperature data by applying a linear ln K_{eq} least-squares analysis according to the van't Hoff equation [Equation (4)].

$$\ln K_{eq} = \frac{-\Delta H}{RT} + \frac{\Delta S}{R} \quad (4)$$

Plots of ln K_{eq} vs. 1/T for different MTO·N systems were linear for all cases studied (Figure 4). The enthalpies and entropies of adduct formation were determined in the usual manner from the slopes and intercepts of the plots and the

Table 3. ΔH, ΔS, and ΔG values for adduct formation of MTO with pyridine derivatives in benzene.

Entry	Ligand	ΔH [kJ mol^{-1}]	ΔS [J K^{-1} mol^{-1}]	ΔG [kJ mol^{-1}][a]
1	pyridine	**–35.1 ± 1.6**	**–65.9 ± 5.3**	**–15.9 ± 0.1**
2	4-picoline	**–34.2 ± 0.1**	**–57.3 ± 0.4**	**–17.4 ± 0.1**
3	3-picoline	**–38.6 ± 1.4**	**–73.2 ± 4.8**	**–17.0 ± 0.1**
4	4-*tert*-butylpyridine	**–31.1 ± 0.6**	**–44.6 ± 1.9**	**–18.1 ± 0.3**
5	methyl nicotinate	**–42.1 ± 0.5**	**–104.1 ± 1.6**	**–11.6 ± 0.2**
6	3,4-dimethylpyridine	**–27.1 ± 5.3**	**–29.0 ± 17.9**	**–18.6 ± 0.2**
7	3-chloropyridine	**–44.1 ± 1.7**	**–113.1 ± 5.7**	**–10.9 ± 0.1**
8	3-phenylpyridine	**–37.0 ± 0.3**	**–74.9 ± 1.1**	**–15.1 ± 0.1**
9	4-benzylpyridine	**–41.2 ± 1.4**	**–83.6 ± 4.5**	**–16.8 ± 0.1**
10	3,5-dibromopyridine	–51.0	–151.4	–6.6
11	4-$Me_2NC_5H_4N$	–19.4	19.9	–25.4
12	3,5-dichloropyridine	–51.5	–154.2	–6.31
13	3-fluoropyridine	–43.3	–109.5	–11.2
14	3-cyanopyridine	–48.8	–139.2	–7.9
15	4-cyanopyridine	–47.3	–131.2	–8.8
16	3-iodopyridine	–42.3	–104.1	–11.8
17	4-phenylpyridine	–34.0	–59.2	–16.7
18	3-methoxypyridine	–36.4	–72.3	–15.3
19	4-methoxypyridine	–30.2	–38.4	–19.0
20	4-phenoxypyridine	–27.8	–27.6	–19.8
21	3-acetylpyridine	–42.5	–105.4	–11.6
22	4-acetylpyridine	–41.3	–99.0	–12.4
23	3-aminopyridine	–32.3	–49.9	–17.7
24	4-aminopyridine	–21.2	10.2	–24.3
25	3-pyridinecarboxyaldehyde	–40.6	–95.3	–12.8
26	4-pyridinecarboxyaldehyde	–42.1	–103.1	–11.9
27	3-nitropyridine	–51.0	–151.6	–6.6
28	4-nitropyridine	–48.2	–136.0	–8.3
29	3-bromo-5-methoxypyridine	–44.6	–116.7	–10.4
30	3-methyl-4-nitropyridine	–46.0	–124.1	–9.6
31	4-amino-3-bromopyridine	–28.6	–30.2	–19.9

[a] At 20 °C.

results are summarized in Table 3. The values of ΔH and ΔS for ligands **1**–**9** were calculated directly from experimental values of K_{eq} and for ligands **10**–**31** they were derived from calculated K_{eq} values at different temperatures. These data allow calculation of the enthalpy and entropy changes for an adduct of any N-donor ligand from its K_{eq} and pK_a. From the data given in Table 3, it is readily obvious that the MTO·N adducts formed in benzene solution are enthalpy stabilized but entropy destabilized. It should be noted that, to the best of our knowledge, no published values of ΔH and ΔS for the adduct formation of MTO are available for comparison with the results obtained here. The ΔG values, calculated from $\Delta G = -RT \ln K_{eq}$ at 20 °C, are included in Table 3.

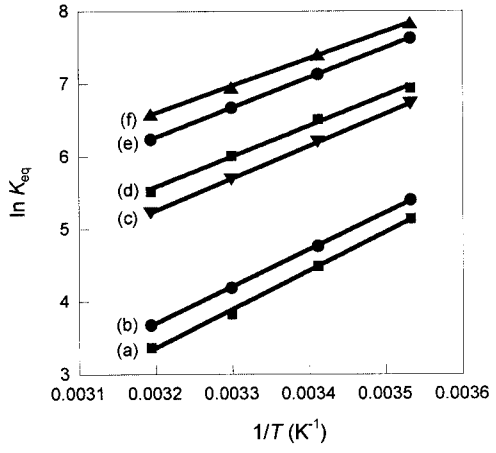

Figure 4. van't Hoff plots for adduct formation of MTO with pyridine derivatives [(a) 3-chloropyridine; (b) methylnicotinate; (c) 3-phenylpyridine; (d) pyridine; (e) 4-methylpyridine; (f) 4-*tert*-butylpyridine] in benzene.

Thermodynamic Analysis of the Adduct-Formation Reaction

Solvation Energy

An Onsager's reaction field model[33–35] was introduced to estimate the solvation energy. The reaction field model expresses solvation energy by

$$\Delta E_{solv} = \frac{2\mu^2}{r^3}\left(\frac{\varepsilon_r - 1}{\varepsilon_r + 2} - \frac{n^2 - 1}{n^2 + 2}\right) \quad (5)$$

where ε_r and n are the dielectric constant and refractive index, respectively, of the solvent and μ and r represent the dipole moment and the diameter, respectively, of the solute. Since the solvent (benzene) is the same for all the systems (MTO + N ⇌ MTO·N), the parentheses term of Equation (5) becomes constant. Thus, solvation energy is assumed to depend only on the μ^2/r^3 term. Since the radii will change only slightly, one can approximate $r_{MTO\cdot N} = r_{MTO}$

+ r_N, and the solvation energy can therefore be expressed as a linear function of μ (see Table 4).

Table 4. Dipole moments of some pyridine derivatives.

Ligand	$\mu_{calcd.}$ [D][a]	$\mu_{exp.}$ [D][b]
Pyridine	2.35	2.20
4-Picoline	2.78	2.68
3-Picoline	2.61	2.45
4-*tert*-Butylpyridine	2.89	
Methyl nicotinate	0.70	
3,4-Dimethylpyridine	3.05	
3-Chloropyridine	2.16	2.02
3-Phenylpyridine	2.48	
4-Benzylpyridine	2.64	

[a] The μ values for N-donors were obtained from B3LYP/6-311++G** calculations with the Gaussian 98 program package.[30] [b] Available experimental data are from refs.[31,32]

For reactions of the type considered in this work $\Delta G = \Delta G^i - \Delta G^s$, where ΔG^i is the Gibbs free energy change of the adduct formation reaction without solvation and ΔG^s is the additional term due to the effect of solvation. We performed a trial plot of ΔG against μ according to Equation (5) for nine different N-donors (**1**–**9**), shown in Figure 5, to determine if there exists any correlation between ΔG (or ΔG^s) and μ. The plot shows a good linear relationship. Therefore, we concluded that ΔG, and hence ΔG^s, are controlled by μ of the N-donor after the reaction field model.

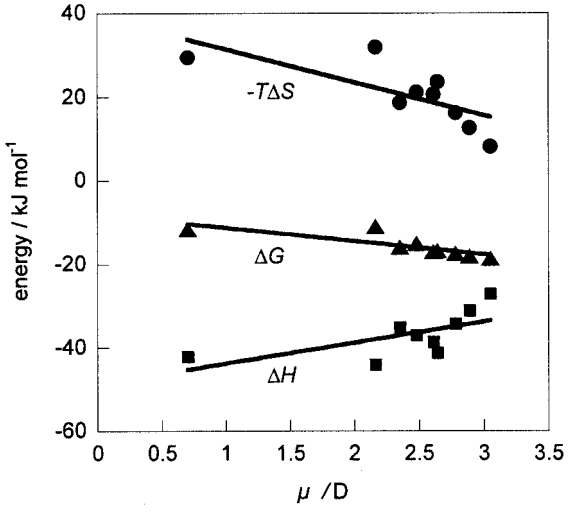

Figure 5. Correlation between ΔH, ΔG, or $T\Delta S$ and dipole moment. Data were taken from Tables 3 and 4 (for ligands **1**–**9**) at 20 °C and fitted to a linear relation.

Enthalpy and Entropy Contributions

The stabilization model by solvation seems to explain the μ-dependence of ΔG in the MTO·N-donor adduct formation. Since the Gibbs free energy consists of enthalpy and entropy terms ($\Delta G = \Delta H - T\Delta S$), we discuss the solvation effect by considering the two terms separately and try to understand how these thermodynamic terms (ΔH and ΔS) of the reaction depend on the dipole moment of the N-donors.

For a given reaction, the enthalpy and entropy changes can be considered to be composed of intrinsic (ΔH^i and ΔS^i) and solvation (ΔH^s and ΔS^s) terms:

$$\Delta H = \Delta H^i + \Delta H^s$$

$$\Delta S = \Delta S^i + \Delta S^s$$

In the enthalpy term, the second term is for the solvation energy and is possibly proportional to μ. We plot the ΔH values against μ in Figure 5 to find some correlation between ΔH and μ. Figure 5 shows a reasonable linear dependence of ΔH upon μ. Therefore, we concluded that ΔH is controlled by μ of the N-donors, and the reaction field model seems valid in the adduct formation MTO + N-donor → Adduct. Since the slope in the plot of ΔH vs. μ is positive, the solvation energy of the reactants is larger than that of the adduct. We discuss this result according to Equation (5). Since the refractive index, n, and the dielectric constant, ε_r, of the solvent are constant, we consider only the μ^2/r^3 term. This formula means that the solvation energy depends on the dipole moment and the volume. We discuss these factors separately. The volumes of MTO and the N-donor are smaller than the adduct, although one can assume that this factor, compare to the dipole moment, is not very important, because $r_{MTO\cdot N} \approx r_{MTO} + r_N$. Thus, the solvation energy for the reactants is larger than that of the adduct. The dipole moment plays an important role in the solvation. The dipole moment of the adduct is probably smaller than the reactants due to the structure of the adduct. The dipoles of MTO and N-donors may be antiparallel and cancel each other out in the adduct. Also, the ΔH value for the adduct MTO·3,4-dimethylpyridine is less negative (–27.1 kJ mol^{-1}) than the others (i.e. MTO·3-ClPy: ΔH = –44.1 kJ mol^{-1}), although the formation constant is the highest (2082.5 L mol^{-1} at 20 °C). It seems that this donor is better solvated, due to its larger dipole moment, and this reduces the overall enthalpy.

The ΔS values, which are negative in the present association reaction, apparently depend on μ and change from –104.1 to –29.0 (J K^{-1} mol^{-1}) as μ increases from 0.7 to 3.05 D, for ligands **5** and **6** respectively. We qualitatively discuss the relation between enthalpy change (ΔH^s) and entropy change (ΔS^s) by solvation. The ΔH values are plotted against ΔS in Figure 6. The absolute value of ΔH (or exothermicity of the reaction) increases as the entropy change decreases, which indicates that solvation controls not only ΔH but also ΔS. When the N-donor has negligibly small μ, the enthalpy changes of solvation ΔH^s for the reactants and the adduct are negligible, and the solvent molecules are loosely bound to the reactants and the adduct. Thus, the solvent molecules are not well aligned with the reactants or with the adduct (negligible ΔS^s). This is the case of the "small μ limit" as shown in the energy diagrams in Figure 7. On the other hand, for the N-donor having large μ, the solvation energy becomes much larger, according to Onsager's reaction field model (negative and larger ΔH^s), and the solvent molecules are tightly trapped by the reactants and the adduct. Thus, the solvent molecules are well aligned

with the reactants and with the adduct (negative and large ΔS^s). This is the case of the "large μ limit" in Figure 7. As a result, the absolute magnitudes of ΔH and ΔS values decrease when μ changes from the small μ limit to the large μ limit. It might be worthy to note that: (1) both ΔH and $T\Delta S$ contribute similarly to ΔG, and that (2) these contributions cancel out each other, resulting in a rather constant ΔG value against μ. This feature is visualized in Figure 5, where ΔG, ΔH, or $-T\Delta S$ are plotted against μ values; the ΔH and $T\Delta S$ contributions vary, but ΔG does not vary greatly for various N-donors with different μ. All these phenomena can be reasonably explained in the thermodynamical terms described above.

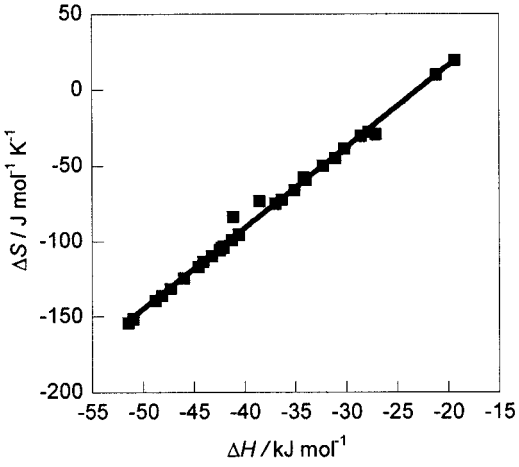

Figure 6. Correlation between ΔH and ΔS (enthalpy–entropy compensation) for adduct formation of MTO with pyridine derivatives. The data are listed in Table 3.

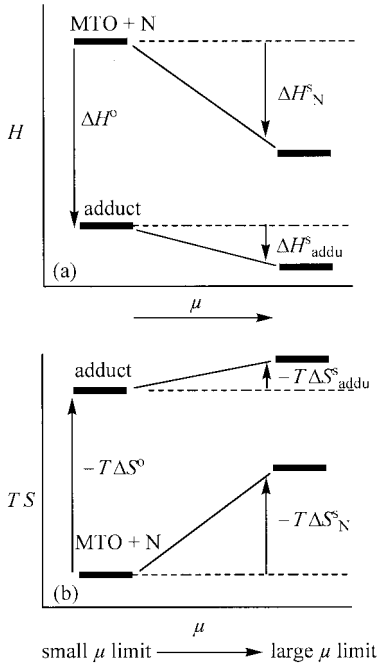

Figure 7. Energy diagrams of the reactants and the adduct: (a) enthalpy changes upon adduct formation; (b) entropy changes upon adduct formation. Both ΔH and $T\Delta S$ are small for N-donors with large μ.

The enthalpy–entropy compensation plot of adduct formation of MTO with pyridine derivatives, which is shown in Figure 6, gives a good straight line. This may be taken as evidence for the operation of a common structure–activity relationship in this series of complexes.[36,37]

Conclusions

Lewis-base adducts of MTO are known to be more rigid at lower temperatures and less strongly coordinated at higher temperatures. The stability of the adducts formed by pyridine and its derivatives with MTO is entirely due to a negative ΔH, while ΔS counteracts the adduct formation investigated here. ΔH and ΔS are controlled by the dipole moments of pyridine derivatives. Both ΔH and ΔS are small for N-donors with large μ.

Experimental Section

The compound methyltrioxorhenium ($MeReO_3$ or MTO) was synthesized according to a literature procedure.[22] The pyridine derivatives were purchased from commercial sources (Merck or Fluka) and were used as received. Benzene (Merck, quality: for spectroscopy) was used as solvent throughout this study and the data were obtained at different temperatures (10, 20, 30, and 40 °C). A Perkin–Elmer Lambda 25 spectrophotometer with temperature control using an EYELA NCB-3100 constant temperature bath was used to record UV/Vis spectra. Typically, a 2×10^{-4} M solution of the MTO in benzene contained in a quartz cuvette with a 1-cm path length was treated with successive aliquots of a solution of the N-donor ligand, of known concentration, in the same solvent. The values of stability constants and the extinction coefficient of adducts at different wavelengths were determined by fitting the equilibrium absorbance to Equation (2) by the method of nonlinear least-squares.

Acknowledgments

We thank the Shiraz University Research Council, Iran (Grant No. 82-SC-1664-C259) for financial support. We also thank Dr. Ghatee for his key help in purchasing the UV/Vis spectrometer.

[1] W. A. Herrmann, R. W. Fischer, D. W. Marz, *Angew. Chem. Int. Ed. Engl.* **1991**, *30*, 1638–1641.
[2] W. A. Herrmann, R. W. Fischer, W. Scherer, M. U. Rauch, *Angew. Chem. Int. Ed. Engl.* **1993**, *32*, 1157–1160.
[3] W. A. Herrmann, J. P. Zoller, R. W. Fischer, *J. Organomet. Chem.* **1999**, *579*, 404–407.
[4] T. H. Zauche, J. H. Espenson, *Inorg. Chem.* **1998**, *37*, 6827–6831.
[5] W. Adam, W. A. Herrmann, J. Lin, C. R. Saha-Möller, R. W. Fischer, J. D. G. Correia, *Angew. Chem. Int. Ed. Engl.* **1994**, *33*, 2475–2476.
[6] W. R. Thiel, R. W. Fischer, W. A. Herrmann, *J. Organomet. Chem.* **1993**, *459*, C9-C11.
[7] W. A. Herrmann, J. D. G. Correia, F. E. Kühn, G. R. J. Artus, C. C. Romão, *Chem. Eur. J.* **1996**, *2*, 168–173.
[8] W. A. Herrmann, R. W. Fischer, M. U. Rauch, W. Scherer, *J. Mol. Catal.* **1994**, *86*, 243–266.

[9] J. Rudolph, K. L. Reddy, J. P. Chiang, K. B. Sharpless, *J. Am. Chem. Soc.* **1997**, *119*, 6189–6190.
[10] H. Adolfsson, A. Converso, K. B. Sharpless, *Tetrahedron Lett.* **1999**, *40*, 3991–3994.
[11] C. Copéret, H. Adolfsson, K. B. Sharpless, *J. Chem. Soc., Chem. Commun.* **1997**, 1565–1566.
[12] W. A. Herrmann, H. Ding, R. M. Kratzer, F. E. Kühn, J. J. Haider, R. W. Fischer, *J. Organomet. Chem.* **1997**, *549*, 319–322.
[13] W. A. Herrmann, F. E. Kühn, M. R. Mattner, G. R. J. Artus, M. Geisberger, J. D. G. Correia, *J. Organomet. Chem.* **1997**, *538*, 203–209.
[14] H. Adolfsson, C. Copéret, J. P. Chiang, A. K. Yudin, *J. Org. Chem.* **2000**, *65*, 8651–8658.
[15] W. D. Wang, J. H. Espenson, *J. Am. Chem. Soc.* **1998**, *120*, 11 335–11 341.
[16] F. E. Kühn, A. M. Santos, P. W. Roesky, E. Herdtweck, W. Scherer, P. Gisdakis, I. V. Yudanov, C. Di Valentin, N. Rösch, *Chem. Eur. J.* **1999**, *5*, 3603–3615.
[17] P. Ferreira, W. M. Xue, É. Bencze, E. Herdtweck, F. E. Kühn, *Inorg. Chem.* **2001**, *40*, 5834–5841.
[18] A. M. Santos, F. E. Kühn, W. M. Xue, E. Herdtweck, *J. Chem. Soc., Dalton Trans.* **2000**, 3570–3574.
[19] S. M. Nabavizadeh, *Inorg. Chem.* **2003**, *42*, 4204–4208.
[20] F. E. Kühn, A. Scherbaum, W. A. Herrmann, *J. Organomet. Chem.* **2004**, *689*, 4149–4164.
[21] B. S. Lane, K. Burgess, *Chem. Rev.* **2003**, *103*, 2457–2473.
[22] W. A. Herrmann, in *Applied Homogeneous Catalysis with Organometallic Compounds* (Eds.: B. Cornils, W. A. Herrmann), 2nd ed., vol. 3, Wiley-VCH, Weinheim, **2002**, p. 1319.
[23] W. A. Herrmann, F. E. Kühn, *Acc. Chem. Res.* **1997**, *30*, 169–180.
[24] W. A. Herrmann, J. G. Kuchler, G. Weichselbaumer, E. Herdtweck, P. Kiprof, *J. Organomet. Chem.* **1989**, *372*, 351–370.
[25] W. A. Herrmann, G. Weichselbaumer, E. Heerdtweck, *J. Organomet. Chem.* **1989**, *372*, 371–389.
[26] C. C. Romão, F. E. Kühn, W. A. Herrmann, *Chem. Rev.* **1997**, *97*, 3197–3246.
[27] R. M. Smith, A. E. Martell, *Critical Stability Constants*, Plenum Press, New York, **1974**.
[28] *CRC Handbook of Chemistry and Physics* (Editor-in-Chief: D. R. Lide), 81st ed., CRC Press, Boca Raton, FL, **2000**.
[29] H. Rudler, J. R. Gregorio, B. Denise, J. M. Brégeault, A. Deloffre, *J. Mol. Catal. A* **1998**, *133*, 255–265.
[30] M. J. Frisch, G. W. Trucks, H. B. Schlegel, G. E. Scuseria, M. A. Robb, J. R. Cheeseman, V. G. Zakrzewski, J. A. Montgomery Jr., R. E. Stratmann, J. C. Burant, S. Dapprich, J. M. Millam, A. D. Daniels, K. N. Kudin, M. C. Strain, O. Farkas, J. Tomasi, V. Barone, M. Cossi, R. Cammi, B. Mennucci, C. Pomelli, C. Adamo, S. Clifford, J. Ochterski, G. A. Petersson, P. Y. Ayala, Q. Cui, K. Morokuma, D. K. Malick, A. D. Rabuck, K. Raghavachari, J. B. Foresman, J. Cioslowski, J. V. Ortiz, A. G. Baboul, B. B. Stefanov, G. Liu, A. Liashenko, P. Piskorz, I. Komaromi, R. Gomperts, R. L. Martin, D. J. Fox, T. Keith, M. A. Al-Laham, C. Y. Peng, A. Nanayakkara, C. Gonzalez, M. Challacombe, P. M. W. Gill, B. Johnson, W. Chen, N. W. Wong, J. L. Andres, M. Head-Gordon, E. S. Replogle, J. A. Pople, Gaussian 98, Revision A.7, Gaussian, Inc., Pittsburgh, PA, **1998**.
[31] I. Pápai, G. Jancsó, *J. Phys. Chem. A* **2000**, *104*, 2132–2137.
[32] V. V. Prezhdo, E. V. Vaschenko, O. V. Prezhdo, A. Puszko, *J. Mol. Struct.* **1998**, *471*, 127–137.
[33] L. Onsager, *J. Am. Chem. Soc.* **1936**, *58*, 1486–1493.
[34] J. N. Wilson, *Chem. Rev.* **1939**, *25*, 377–406.
[35] E. G. McRae, *J. Phys. Chem.* **1957**, *61*, 562–572.
[36] L. Liu, Q. X. Guo, *Chem. Rev.* **2001**, *101*, 673–696.
[37] J. H. Espenson, *Chemical Kinetics and Reaction Mechanisms*, McGraw-Hill, New York, 2nd ed., **1995**.

Received: January 04, 2005

